Self-consistent LCAO-CPA method for disordered alloys

Klaus Koepernik, B. Velický,* Roland Hayn, and Helmut Eschrig
MPG Research Group Electron Systems, Department of Physics, TU Dresden, D-01062, Dresden, Germany
(Received 9 August 1996)

We present a scheme for calculating the electronic structure of disordered alloys, self-consistent in the local-density-approximation sense. It is based on expanding the one-electron Green's function in the basis of modified atomic orbitals [H. Eschrig, *Optimized LCAO Method and the Electronic Structure of Extended Systems* (Springer, Berlin, 1989)]. The two-terminal approximation introduced for the Hamiltonian and the overlap matrix permits us to treat both the diagonal and off-diagonal disorder using an extension of the Blackman-Esterling-Berk form of the coherent-potential approximation (CPA) [Phys. Rev. B **4**, 2412 (1971)] to a nonorthogonal basis set. Calculations using the scalar relativistic density functional for the magnetic binary transition-metal alloys Fe-Co, Fe-Pt, Co-Pt, and for the ternary alloy Al-Fe-Mn give results comparing well with experimental data and calculations based on the Korringa-Kohn-Rostoker (KKR)-CPA and linear muffin-tin orbital-CPA techniques. [S0163-1829(97)03509-1]

I. INTRODUCTION

Several powerful implementations of the coherent-potential approximation[1–3] (CPA) to calculate the electronic structure of substitutional alloys have been developed in recent years. Early applications of the CPA with first-principles band-structure methods were mostly based on the method of Korringa, Kohn, and Rostoker (KKR),[4] and this KKR-CPA is still widely used, e.g., Ref. 5. In view of the multiple-scattering formulation underlying the KKR theory, the incorporation of the CPA turns out to be quite natural.

To reduce the numerical effort of the KKR method, the tight-binding-linear-muffin-tin-orbital[6] (TB-LMTO) method was developed. Another linear band-structure scheme is the linear-combination-of-atomic-orbitals (LCAO).[7] To incorporate the CPA idea into these linear band-structure methods one has to start from an algebraic, matrix version of the CPA instead of using the multiple-scattering language. In this way, a TB-LMTO-CPA (Ref. 8) was developed and also first steps towards a LCAO-CPA (Refs. 9–11) were made. These approaches made it possible to apply the CPA in quite complex structures like multilayers, surfaces or interfaces[12] or in bulk materials with complex unit cells and partial disorder. First TB-LMTO-CPA calculations on partially disordered alloys were performed by Kudrnovský *et al.*,[13,14] however not fully charged and spin self-consistent. Recently, the screened KKR approach was introduced.[15] It combines the pleasant features of a TB formulation with the rigorousness of a multiple-scattering approach.

In the past, special attention has been drawn to the problem of off-diagonal disorder appearing in the matrix CPA. In the case of multiplicative off-diagonal disorder one can use the approach proposed by Shiba,[16] which was introduced into the TB-LMTO-CPA.[17–19] For the case of general off-diagonal disorder the procedure of Blackman-Esterling-Berk[20] (BEB) is applicable. Some applications of BEB to band-structure calculations were reported in Ref. 21 using a tight-binding fit. But to the authors' knowledge, the BEB approach was never used in a first-principles, charge self-consistent CPA application.

Within the LCAO scheme one deals with a nonorthogonal basis. There have been attempts to implement the CPA in nonorthogonal basis schemes.[9–11] However, up to now there were no charge self-consistent calculations and the off-diagonal disorder was only treated in virtual crystal approximation (VCA). Despite the many similarities between LCAO and TB-LMTO there are also some differences. LCAO puts no restriction on the shape of the potential, as for instance the atomic-sphere approximation (ASA) of the TB-LMTO-CPA.

Our aim will be to present a fully charge self-consistent approach to complex lattices based on a nonorthogonal LCAO basis scheme without restriction to VCA. We will treat all randomness of the Hamiltonian and of the overlap matrix including off-diagonal disorder at the same level. The approach is applicable to a wide class of alloys. It is based on a pseudospin description often used in the past (in the BEB theory,[20] in the augmented space method[22]). We present a generalization of the BEB theory to sublattices and to nonorthogonal basis sets in the propagator formalism, embedded in a charge self-consistent treatment. A variant of a propagator formalism for BEB was proposed, for example, in Ref. 23, where the analyticity of the BEB Green's function was proved. In the context of the propagator formalism we present a formulation of the full multiple-scattering problem within the LCAO approach comparable to the KKR description. This leads to a quite natural introduction of the single-site approximation.

The problem of disordered alloys naturally requires quite a number of approximations. In our opinion two points have to be met by every charge self-consistent CPA method. It should incorporate the major effects of disorder at least in single-site mean-field approach and rely on a band-structure scheme which is sufficiently accurate in relation to the accuracy of the CPA. When using a wave-function approach, the possibility of a single-site approximation implies the use of not only a local but an effectively well localized basis. In the TB-LMTO this is achieved by the additional LMTO-TB transformation, which is not entirely without problems. The optimized local orbital approach,[7] approved for ordered

structures, seems to us particularly appropriate to a more direct solution. It leads naturally to the terminal-point approximation and therefore includes the most general kind of off-diagonal disorder. Clearly the mean-field treatment of the disorder via single-site CPA has a quite strong model character. However, in the case of a BEB theory the randomness of the environment is taken into account at least with respect to the two terminal points of all matrices, thus giving a good description of the densities of states as demonstrated for model systems. Our combination of the CPA with the nonorthogonal LCAO fulfills the requirement with respect to the accuracy of the whole scheme and thereby arrives directly at a matrix representation without a tight-binding transformation of the Hamiltonian.

Our paper is organized as follows. First, in Sec. II, we present the representation of the charge density of an alloy in terms of conditionally averaged Green's functions and local orbitals. This is necessary to obtain the self-consistent potential in the spirit of the local-density approximation (LDA). Next, in Sec. III, we generalize the BEB theory to nonorthogonal basis sets and to the case of several sublattices in terms of the propagator formalism. In Section IV we describe the numerical procedure and present the underlying equations. In Sec. V we apply the method to binary and ternary transition-metal alloys. The binary examples FeCo and especially CoPt and FePt prove the applicability and accuracy of our approach to alloys with a great difference in the bandwidths of the constituents and to cases where relativistic effects are important. The last example FeMnAl is a rather complex one. It shows a rich structure of the magnetic phase diagram. Here we present an investigation of the ferromagnetic phase. In that case, we obtain magnetic moments in agreement with experiment for all Al concentrations, however, at higher Al content, the incorporation or partial order is decisive in obtaining agreement with experiment. We discuss the dependence of the moments on the local environment.

II. KOHN-SHAM APPROACH TO ALLOYS IN LOCAL ORBITAL REPRESENTATION

Theoretically, an alloy is described as an ensemble of configurations of atoms, accompanied with the definition of an average of observable quantities. For each configuration, in the spirit of density-functional theory an effective single-particle Hamiltonian is introduced, depending on the electron density of that configuration. Instead of summing over the squares of Kohn-Sham orbitals, in alloy theory it is preferable to use the single-particle Green's function in closing the self-consistency cycle.

A. Local orbital representation of the single-particle Green's function

Given an atomic configuration, the Kohn-Sham theory starts from an effective single-particle Hamiltonian (we use atomic units $\hbar = m_e = |e| = 1$):

$$H(\vec{r}) = -\frac{1}{2}\Delta + V(\vec{r}) \quad . \tag{1}$$

with the potential being a function of atomic species and positions and a functional of the electron density. The ground-state electron density is again solely determined by the atomic species and positions. For the sake of simplicity in the notation, a possible spin dependence is understood in the following without mention. In a relativistic version, a Pauli Hamiltonian or a Dirac Hamiltonian can be used likewise. To prepare for the alloy case we define the retarded single-particle Green's function in real space ($\omega^+ = \omega + i\delta$):

$$[\omega^+ - H(\vec{r})]G(\vec{r},\vec{r}';\omega^+) = \delta(\vec{r}-\vec{r}') \quad . \tag{2}$$

From its imaginary part the electron density may be calculated as

$$n(\vec{r}) = -\frac{1}{\pi}\int \mathrm{Im}G(\vec{r},\vec{r};\omega^+)\Theta(\varepsilon_\mathrm{F}-\omega)d\omega \quad , \tag{3}$$

where Θ is the step function and ε_F denotes the Fermi level.

At this stage we introduce a nonorthogonal local orbital representation[7] of all real-space quantities. The basis orbitals are classified as valence $|i\mu)$ and core $|ic)$ states with site index i and atomic quantum numbers μ and c, respectively. The core states are assumed to be nonoverlapping and orthogonal to each other, while the valence states are not. To get rid of the core part of the Hamiltonian, we project the valence basis states onto the Hilbert subspace orthogonal to all core states:

$$|i\mu\rangle = |i\mu) - \sum_{lc} |lc)(lc|i\mu) \quad . \tag{4}$$

Core states and the corresponding density contributions are separately treated as a first step in each cycle of self-consistency.

From now on, we consider the valence subspace in the Hilbert space which in practical implementations is spanned by a finite number of basis states per site, but is sufficiently complete to represent the occupied valence eigenstates. All following quantities like Hamiltonian, overlap matrix, and Green's function will be given as projected to this subspace. It may likewise be considered as spanned by a set of orthonormalized states $|k\rangle$ containing the occupied eigenstates of the projected Hamiltonian:

$$|k\rangle = \sum_{i\mu} |i\mu\rangle a^k_{i\mu} \quad , \tag{5}$$

$$1_{\mathrm{valence}} = \sum_k |k\rangle\langle k| = \sum_{\substack{i\ \mu \\ i'\mu'}} |i\mu\rangle \sum_k a^k_{i\mu} a^{k*}_{i'\mu'} \langle i'\mu'| \quad . \tag{6}$$

In practical implementations, completeness in this sense is checked as basis set convergence. The coefficients $a^k_{i\mu}$ define the valence states and the inverse of the overlap matrix S:

$$\sum_k a^k_{i\mu} a^{k*}_{i'\mu'} = \langle i\mu|i'\mu'\rangle^{-1} = S^{-1}_{i\mu,i'\mu'} \quad . \tag{7}$$

Straightforwardly we deduce the Hamiltonian matrix, the overlap matrix, and from Eq. (2) the Green's matrix (see also Ref. 9):

$$H(\vec{r})=\sum_{\substack{i\mu i'\mu'\\ j\nu j'\nu'}}\langle\vec{r}|j\nu\rangle S^{-1}_{j\nu,i\mu}\langle i\mu|H(\vec{r})|i'\mu'\rangle \times S^{-1}_{i'\mu',j'\nu'}\langle j'\nu'|\vec{r}\rangle \ ,$$

$$H=\|\langle i\mu|H(\vec{r})|i'\mu'\rangle\| \ ,$$

$$S=\|\langle i\mu|i'\mu'\rangle\| \ ,$$

$$1=(\omega^{+}S-H)G^{+} \ . \tag{8}$$

$G^{\pm}$ abbreviates $G(\omega^{\pm})=G(\omega\pm i\delta)$.

The contravariant Green's matrix elements in the nonorthogonal basis are defined as

$$G^{\pm}_{i\mu,i'\mu'}\equiv\sum_{\substack{j\nu\\ j'\nu'}} S^{-1}_{i\mu,j\nu}\langle j\nu|G(\vec{r},\vec{r}';\omega^{\pm})|j'\nu'\rangle S^{-1}_{j'\nu',i'\mu'} \ . \tag{9}$$

Starting from the Kohn-Sham ansatz the valence part of the electron density is given by

$$n(\vec{r})=\sum_{k}\langle\vec{r}|k\rangle\Theta(\varepsilon_{\mathrm{F}}-\varepsilon_k)\langle k|\vec{r}\rangle \ , \tag{10}$$

where ε_{F} again denotes the Fermi energy. (The core part has a similar structure and will be added, but it is simple and is not the object of consideration here.) We replace the Θ function by an integral over a δ function, which is expressed as the difference of the retarded and advanced one-particle Green's functions. After switching to the local basis (4) we get

$$n(\vec{r})=-\frac{1}{2\pi i}\sum_{\substack{i\mu\\ i'\mu'}}\langle\vec{r}|i\mu\rangle\int^{\varepsilon_{\mathrm{F}}}d\omega \times[G^{+}-G^{-}]_{i\mu,i'\mu'}\langle i'\mu'|\vec{r}\rangle \ . \tag{11}$$

The involved integration starts below the band bottom of the valence states. The occurrence of the advanced Green's matrix is due to moving the imaginary part in Eq. (3) between the (possibly complex) local basis states. [In cases of a real Hamiltonian matrix—in the presence of inversion symmetry—the difference in Eq. (11) reduces to the imaginary part of the retarded Green's matrix.] To simplify the notation, we use the abbreviation $\mathrm{Im}G\equiv 1/2i(G^{+}-G^{-})$ in the following. We get a density representation consisting of (overlapping) local site densities (for $i=i'$) and of doubly terminated terms called overlap density:

$$n(\vec{r})=-\frac{1}{\pi}\sum_{i\mu,i'\mu'}\langle\vec{r}|i\mu\rangle\int^{\varepsilon_{\mathrm{F}}}\mathrm{Im}G_{i\mu,i'\mu'}d\omega\langle i'\mu'|\vec{r}\rangle \ . \tag{12}$$

Up to this point we considered a given configuration of an alloy. One of the main problems here is the lack of periodicity, so that there are no good quantum numbers characterizing the eigenstates $|k\rangle$ of the Hamiltonian. To arrive at measurable quantities, we have to carry out a configurational average.

We want to point out that we have no frozen-core treatment, since in this approach it would not lead to a simplification. In each cycle of charge self-consistency the core states and the projected valence basis states will be recalculated.

B. Pseudospin description of the ensemble

In this paper we discuss substitutional disordered alloys, taking into account the possibility of a complex unit cell. The vectors of the underlying lattice will be denoted by $\vec{R}$ and the basis vectors by $\vec{s}$. Each site belongs to a sublattice. The sublattices may be randomly occupied by various species of atoms or by a vacancy. Each alloy configuration is mapped onto a set of pseudospins $\{\eta^{Q}_{\vec{R}\vec{s}}\}$:

$$\eta^{Q}_{\vec{R}\vec{s}}=\begin{cases}1, & \text{atom of species } Q \text{ at } \vec{R}+\vec{s}\\ 0, & \text{otherwise,}\end{cases} \qquad \sum_{Q}\eta^{Q}_{\vec{R}\vec{s}}=1 \ , \tag{13}$$

(''species'' may include vacancy). Many physical properties of interest are defined as configurational averages denoted in the following by $\langle\cdots\rangle$. Applying it we introduce the concentration of the species Q with respect to a specified site $\vec{s}$ in the unit cell:

$$\langle\eta^{Q}_{\vec{R}\vec{s}}\rangle=c^{Q}_{\vec{s}}\Rightarrow\sum_{Q}c^{Q}_{\vec{s}}=1 \tag{14}$$

and the condition of statistical independence of all sites:

$$\langle\eta^{Q}_{\vec{R}\vec{s}}\,\eta^{Q'}_{\vec{R}'\vec{s}'},\rangle=c^{Q}_{\vec{s}}\,c^{Q'}_{\vec{s}'} \quad \text{for } \vec{R}+\vec{s}\neq\vec{R}'+\vec{s}' \ . \tag{15}$$

For the sake of simplicity, we use in the following a multiple index $i=\vec{R}\vec{s}$.

We construct now the local orbitals for an alloy with the help of those stochastic pseudospins:

$$|i\mu)=\sum_{Q}|iQ\mu)\,\eta^{Q}_{i}, \quad \text{local stochastic valence basis}, \tag{16}$$

$$|ic)=\sum_{Q}|iQc)\,\eta^{Q}_{i}, \quad \text{local stochastic core states}. \tag{17}$$

The pseudospin ensures that the correct basis state is used at the right place. The orthogonalization to core states corresponds to the ''Q expanded'' equation (4):

$$|i\mu\rangle=\sum_{Q}|iQ\mu\rangle\,\eta^{Q}_{i}, \tag{18}$$

$$|iQ\mu\rangle = |iQ\mu) - \sum_{lcQ'} |lQ'c)\,\eta_l^{Q'}(lQ'c|iQ\mu) \quad . \tag{19}$$

The core states fulfill the relation:

$$\eta_i^Q(iQc|i'Q'c')\,\eta_{i'}^{Q'} = \delta_{ii',QQ',cc'}\,\eta_i^Q \quad , \tag{20}$$

since for $i \neq i'$ and for $i = i'$, $Q = Q'$ they are orthonormal, and $\eta_i^Q \eta_i^{Q'} = \delta_{QQ'}$ at a given site i by definition (13).

To employ the pseudospin representation, we introduce the Q-expanded expression (12) for the density:

$$n(\vec{r}) = -\frac{1}{\pi} \sum_{iQ\mu,i'Q'\mu'} \langle \vec{r}|iQ\mu\rangle \times \int^{\varepsilon_F} \mathrm{Im}[\,\eta_i^Q G_{i\mu,i'\mu'}(\omega)\,\eta_{i'}^{Q'}]\,d\omega \langle i'Q'\mu'|\vec{r}\rangle \quad . \tag{21}$$

We interpret the η product of the Green's function as a new quantity, the expanded Green's matrix:

$$\underline{G}_{i\mu,i'\mu'}^{QQ'} = \eta_i^Q G_{i\mu,i'\mu'}\,\eta_{i'}^{Q'} \, . \tag{22}$$

The definition (22) gives the key quantity for the introduction of the BEB transformation in Sec. III.

C. Conditional average of the charge density

The expanded expression (21) for the charge density is suitable for configuration averaging, yielding the average over the whole alloy ensemble:

$$n(\vec{r}) = -\frac{1}{\pi} \sum_{iQ\mu,i'Q'\mu'} \langle \vec{r}|iQ\mu\rangle \times \int^{\varepsilon_F} \mathrm{Im}\langle\, \eta_i^Q G_{i\mu,i'\mu'}(\omega)\,\eta_{i'}^{Q'}\rangle\, d\omega \langle i'Q'\mu'|\vec{r}\rangle \, . \tag{23}$$

Herein the Green's matrix appears in a new context. The twofold conditional average of the η multiplied matrix is the commonly used projected Green's function.[17] To calculate an ensemble average of the density, first the stochastic expression (21) is reduced to a sum of twofold conditionally averaged terms, that means insertion of the two-site conditional averages of Eq. (22) in Eq. (21).

Now we proceed to the basic step which will permit the use of the single-site approximation, namely we will approximate the actual two-terminal elements of the Green's matrix (22) by their conditional component projected configuration averages:

$$\eta_i^Q \langle\, \eta_i^Q G_{i\mu,i'\mu'}\,\eta_{i'}^{Q'}\rangle_{\substack{Q\to i\\ Q'\to i'}}\,\eta_{i'}^{Q'} \, . \tag{24}$$

$\langle\cdots\rangle_{\substack{Q\to i\\ Q'\to i'}}$ means averaging over all members of the ensemble of configurations with fixed occupation at the two terminal points: $\eta_i^Q = \eta_{i'}^{Q'} = 1$. Hence, Eq. (24) differs from Eq. (22) by configuration averaging over all sites, except i and i'. These averages are self-averaging, so that all random environment effects are neglected. The matrix elements (24) still contain a stochastic dependence on two sites. To arrive finally at the single-site description of an alloy, we are led to a corresponding assumption about the form of the density used in the self-consistency cycle:

$$n(\vec{r}) \approx \sum_{iQ} \eta_i^Q n_i^Q \, . \tag{25}$$

This means the full charge density for a configuration shall be additively decomposed into single-site components. These will be replaced by the self-averaging component projected densities given by ensemble averages. Thus we neglect the two-site correlated fluctuations in the local densities. An additional average over the right index of the overlap elements in Eq. (24) serves to reduce Eq. (21) to a sum of single-site expressions:

$$n_i^Q(\vec{r}) = -\frac{1}{\pi} \sum_{i'Q'\mu\mu'} \langle \vec{r}|iQ\mu\rangle \times \int^{\varepsilon_F} \mathrm{Im}\langle \underline{G}_{i\mu,'\mu'}^{QQ'}\rangle_{\substack{Q\to i\\ Q'\to i'}} d\omega \langle i'Q'\mu'|\vec{r}\rangle \times [\,\delta_{ii'} + (1-\delta_{ii'})c_{i'}^{Q'}] \, . \tag{26}$$

Expression (26) gives the alloy version of the local charge-density contribution used in Ref. 7 to recalculate the crystal potential.

D. Site decomposition of the random self-consistent potential

To close the self-consistency cycle we have to calculate the potential $V(\vec{r})$ from the density (25). In the spirit of the single-site approximation and in correspondence with Eq. (25), we have to make an ansatz for the configuration dependence of the potential: we assume it to be a sum of local terms of unspecified shapes, but Q dependent and linearly depending on the pseudospin:

$$V(\vec{r}) = \sum_Q \eta_{\vec{R}\vec{s}}^Q V_{\vec{s}}^Q(\vec{r} - \vec{R} - \vec{s}) \, . \tag{27}$$

This is of course a single-site approximation, there is however no approach available which goes beyond it, except for extremely costly direct simulations of an ensemble of configurations or cluster calculations, which would reach far beyond the single-site picture. Recall that every charge and spin self-consistent single-site CPA approach is bound to express the site potential by the site density alone. However, at variance with KKR or LMTO, here the overlap of site densities and potentials is not at all restricted. The actual potential construction from the density is described consisting of two parts, constructing the Coulomb contribution and the exchange and correlation contribution.

Once one has calculated the electron density as a sum of local overlapping site densities one proceeds as follows. The charge contribution contained in $n_{\vec{s}}^Q(\vec{r})$ amounts to

$$A_{\vec{s}}^Q = \int n_{\vec{s}}^Q(\vec{r})\,d\vec{r} \, . \tag{28}$$

Together with the nuclear charge $Z_{\vec{s}}^Q$ we divide the total charge density around atom $\vec{s}$ in a neutral part and an ionic point charge:

$$\underbrace{\left(A_{\vec{s}}^Q \delta(\vec{r}) - n_{\vec{s}}^Q(\vec{r})\right)}_{\text{neutral}} + \underbrace{\left(Z_{\vec{s}}^Q - A_{\vec{s}}^Q\right)\delta(\vec{r})}_{\text{ionic}} . \tag{29}$$

The neutral part gives rise to localized but overlapping Coulomb potential wells via Poisson's equation. We assume as usually in solid-state physics local charge neutrality. That means that any ionicity must be totally screened within a certain cluster range. Since we have no detailed information on that screening in an alloy, we simply use a Gaussian screening[7] within a range p^{-1}, i.e., we combine the ionic point charge $I_{\vec{s}}^Q = Z_{\vec{s}}^Q - A_{\vec{s}}^Q$ with a Gaussian screening charge according to

$$I_{\vec{s}}^Q \left(\delta(\vec{r}) - \frac{p^3}{\pi^{3/2}} e^{-p^2 r^2} \right) . \tag{30}$$

The screening length p has to be chosen such that the lattice sum of the added heavily overlapping Gaussian charge densities is essentially zero. This treatment is comparable to the discussion in the literature. In Refs. 24 and 25 a screened impurity model is used to describe the effect of the Madelung potential in a disordered alloy. It is based on the observation that almost all of the compensating charge is located in the first coordination shell around the impurity.

The exchange and correlation potential which is less sensitive to density modulations is calculated in an ASA approximation:

$$V_{\text{xc},\vec{s}}^Q \left[n_{\vec{s}}^Q + \sum_{\vec{R}' + \vec{s}' \neq \vec{s}, Q'} c_{\vec{s}'}^{Q'} n_{\vec{R}'\vec{s}'}^{Q'} \right](\vec{r})$$
$$\text{for } |\vec{r}| \leqslant r_{\text{ASA},\vec{s}}^Q , \tag{31}$$

$$V_{\text{xc, interstitial}} = \text{const} \quad \text{for} \quad |\vec{r}| > r_{\text{ASA},\vec{s}}^Q . \tag{32}$$

This latter simplification used in our applications of Sec. V is however not a necessary prerequisite of the approach. By this we complete the charge and spin self-consistency cycle, provided the average of the Green's matrix (22) is obtained.

III. THE COHERENT-POTENTIAL APPROXIMATION

The preceding section was devoted to the construction of the self-consistent potential from a known Green's function in the orbital representation. Now, we come to the other part, namely to the approximate calculation of the corresponding Green's matrix. This is an algebraic problem. Thus, unlike in the KKR approach, the multiple-scattering problem is solved in the corresponding arithmetic space, rather than in the real space.[9] We have to make the fundamental two-terminal approximation. Then, the structure of the Green's matrix (22) and the requirement to treat both the Hamiltonian and the overlap matrix in the same manner without neglecting off-diagonal disorder leads naturally to the BEB theory.

A. Algebra of pseudospins and the Blackman-Esterling-Berk formalism

In Sec. II B we introduced the pseudospins. Now we give them an algebraic structure, which leads in consequence to the BEB transformation. For a given site i, the pseudospin η_i^Q is a column indexed by Q. For the following, it is advantageous to consider it as a diagonal block of a rectangular matrix $\eta = \| \eta_i^Q \delta_{ii'} \|$, to be used together with its transposed η^T in the definition of configuration-dependent projectors χ:

$$\chi \equiv \eta \eta^T, \quad \eta^T \chi = \eta^T, \quad \chi \eta = \eta . \tag{33}$$

This χ is simply a square diagonal matrix with diagonal elements $\chi_{ii}^{QQ} = \eta_i^Q$ of Eq. (13). It has the properties

$$\chi^2 = \chi, \quad \text{Tr}_Q \chi_{ii'} = \delta_{ii'} . \tag{34}$$

We expand the Hamiltonian and overlap matrices to contain information of all possible configurations in such a way that the formerly introduced matrices of a given configuration are obtained by projection:

$$H = \left\| \sum_{QQ'} \eta_i^Q \langle iQ\mu | H(\vec{r}) | i'Q'\mu' \rangle \eta_{i'}^{Q'} \right\| = \eta^T \underline{H} \eta \ , \tag{35}$$

$$S = \left\| \sum_{QQ'} \eta_i^Q \langle iQ\mu | i'Q'\mu' \rangle \eta_{i'}^{Q'} \right\| = \eta^T \underline{S} \eta . \tag{36}$$

$\underline{H}$ and $\underline{S}$ are the expanded matrices. (The η's provide a mapping of the product Hilbert space of all configurations onto the valence Hilbert spaces of given configurations. The ''tensor products'' $\chi = \eta \eta^T$, at variance, are projectors within the expanded Hilbert space onto the subspaces corresponding to those configurations. In this sense the BEB theory is a kind of ''tensorial'' CPA. Compare the paper Ref. 26, where a similar language is used in the framework of the KKR-CPA.) It is worth noting that H and S are stochastic and not translational invariant, while $\underline{H}$ and $\underline{S}$ will be approximated in the following by expressions which are no longer stochastic and are translational invariant. This structure is used in the BEB formalism[20] (the x_i and y_i in that paper are the components η_i^A and η_i^B for the binary case).

The pseudospins η enter the matrices H and S in three ways: at the left and right ''matrix terminals,'' and via the crystal potential and the core orthogonalization corrections. We average over the η's entering on sites different from both terminal sites of the matrices. This terminal-point approximation preserves the full η dependence at both terminal sites and is far better than the former virtual-crystal approximation,[9] since the only averaged parts are the crystal-field and the orthogonalization corrections from *third* centers. The expanded matrices are now split into on-site and off-site terms:

$$\underline{H} = \dot{\underline{H}} + \check{\underline{H}}, \quad \dot{\underline{H}} \chi = \chi \dot{\underline{H}} \ , \tag{37}$$

$$\underline{S} = \dot{\underline{S}} + \check{\underline{S}}, \quad \dot{\underline{S}} \chi = \chi \dot{\underline{S}}, \quad \dot{\underline{S}} \approx \underline{1} \ , \tag{38}$$

with the detailed structure:

$$\underline{\dot{S}}^{QQ'}_{i\mu,i'\mu'} \approx \delta_{ii',QQ'}\left[\delta_{\mu\mu'} - \sum_{lcQ}\underline{(iQ\mu|l\overline{Qc})c^{\overline{Q}}_{l}(l\overline{Qc}|iQ\mu')}\right], \tag{39}$$

$$\underline{\check{S}}^{QQ'}_{i\mu,i'\mu'} \approx (1-\delta_{ii'})\left[(iQ\mu|i'Q'\mu') - \sum_{lcQ}\underline{(iQ\mu|l\overline{Qc})c^{\overline{Q}}_{l}(l\overline{Qc}|i'Q'\mu')}\right], \tag{40}$$

$$\underline{\dot{H}}^{QQ'}_{i\mu,i'\mu'} \approx \delta_{ii',QQ'}\left[(iQ\mu|\hat{t}+V^{Q}_{i}|iQ\mu') + \sum_{l\neq i,Q}\underline{(iQ\mu|c^{\overline{Q}}_{l}V^{\overline{Q}}_{l}|iQ\mu')} - \sum_{lcQ}\underline{(iQ\mu|l\overline{Qc})c^{\overline{Q}}_{l}\varepsilon^{\overline{Q}}_{lc}(l\overline{Qc}|iQ\mu')}\right], \tag{41}$$

$$\underline{\check{H}}^{QQ'}_{i\mu,i'\mu'} \approx (1-\delta_{ii'})\left[(iQ\mu|\hat{t}+V^{Q}_{i}+V^{Q'}_{i'}|i'Q'\mu') + \sum_{l\neq i,i',Q}\underline{(iQ\mu|c^{\overline{Q}}_{l}V^{\overline{Q}}_{l}|i'Q'\mu')} - \sum_{lcQ}\underline{(iQ\mu|l\overline{Qc})c^{\overline{Q}}_{l}\varepsilon^{\overline{Q}}_{lc}(l\overline{Qc}|i'Q'\mu')}\right]. \tag{42}$$

The energy levels $\varepsilon^{\overline{Q}}_{lc}$ are the core levels c of atom $\overline{Q}$. The combination of the matrix elements of the three center potential and the core orthogonalization correction at a given site is known as the Phillips-Kleinman pseudopotential.[27] Normally, its action on smooth functions is quite small, so the average over it at third centers away from the basis function centers is not a severe approximation. Now we are prepared to formulate the multiple-scattering theory in the pseudospin language.

B. The scattering problem

The random arrangement of different types of atoms in the disordered alloy and the resulting breaking of the translational symmetry leads to an incoherent scattering of the electrons. By defining a coherent reference medium it is possible to collect all incoherent parts of the scattering with respect to this medium in one quantity, called the scattering matrix T. Then the Green's function of the disordered alloy is expressed in terms of the propagation in the coherent medium and of the scattering matrix. The coherent medium will be defined by a self-consistency condition.

We start by Q expanding the equation of motion of the one-particle Green's matrix (8):

$$\eta^{T}(\omega\underline{S}-\underline{H})\,\eta G = 1\,. \tag{43}$$

From Eq. (22) we take the idea to multiply this equation with η on the left and with η^{T} on the right to get an equation of motion for $\underline{\mathcal{G}} = \eta G\,\eta^{T}$:

$$\chi(\omega\underline{S}-\underline{H})\,\eta G\,\eta^{T} = \chi\,. \tag{44}$$

Now we use the definition of χ and the commutation rules in Eqs. (37) and (38):

$$[\omega\underline{\dot{S}}-\underline{\dot{H}}+\chi(\omega\underline{\check{S}}-\underline{\check{H}}]\chi)\,\eta G\,\eta^{T} = \chi\,. \tag{45}$$

When using the vacancy concept we associate at least one basis orbital with every site, sort of a smooth Gaussian at the vacancy site.

Then the expression on the left-hand side is stochastic but Herglotz, so that the resolvent exists in the upper complex ω half plane:

$$\underline{\mathcal{G}} \equiv \eta G\,\eta^{T} = \chi\,\eta G\,\eta^{T} \tag{46}$$

$$= \chi[\omega\underline{\dot{S}}-\underline{\dot{H}}+\chi(\omega\underline{\check{S}}-\underline{\check{H}})\chi]^{-1}\chi$$

$$= \chi\left[\underbrace{\omega\underline{\dot{S}}-\underline{\dot{H}}-\chi\,(\omega-\underline{\Sigma})\,\chi}_{\equiv -\underline{a}} + \chi\underbrace{\left(\omega-\underline{\Sigma}+\omega\underline{\check{S}}-\underline{\check{H}}\right)}_{\equiv \underline{\Gamma}^{-1}}\chi\right]^{-1}\chi\,. \tag{47}$$

Here we introduced the Herglotz $\underline{a}$ (the stochastic potential) and the Herglotz Γ (the nonstochastic nonlocal coherent Green's matrix). The next steps are aimed at collecting all stochastic quantities (χ and $\underline{a}$) into one matrix:

$$\underline{\mathcal{G}} = \chi\left(\chi\underline{\Gamma}^{-1}\chi - \underline{a}\right)^{-1}\chi \;=\; -\left[\underbrace{\chi\underline{a}^{-1}\chi}_{\equiv\,\underline{b}} + \chi\underline{a}^{-1}\chi\underline{\Gamma}^{-1}\chi\underline{a}^{-1}\chi + \cdots\right] \tag{48}$$

$$\underline{\mathcal{G}} = \underline{b}(\underline{b}-\underline{\Gamma})^{-1}\underline{\Gamma} = \underline{\Gamma} + \underline{\Gamma}(\underline{b}-\underline{\Gamma})^{-1}\underline{\Gamma} \equiv \underline{\Gamma} + \underline{\Gamma}\;\underline{T}\;\underline{\Gamma}\,. \tag{49}$$

At this stage we expressed the multiple scattering in terms of the translational invariant coherent Green's matrix $\underline{\Gamma}$ (in the product Hilbert space) and the random perturbation $\underline{b}$.

The averaging procedure now follows the well-known scheme. The nonregular inverse potential $\underline{b}$, containing all randomness, defines the scattering matrix $\underline{T}$, whose average is required to vanish:

$$\langle \underline{T} \rangle = \langle (\underline{b} - \underline{\Gamma})^{-1} \rangle \equiv 0 \Rightarrow \langle \underline{\mathcal{G}} \rangle = \underline{\Gamma} . \tag{50}$$

In that way we defined the self-energy $\underline{\Sigma}$. Remembering our aim we examine some projector relations concerning the two-site conditional average of $\underline{\mathcal{G}}$. From Eq. (46) we deduce

$$\underline{\mathcal{G}} = \chi \underline{\mathcal{G}} \chi, \quad \chi_{ii}^{QQ}|_{q \to i} = \delta_{qQ} , \tag{51}$$

$$\underline{\mathcal{G}}_{ii'}^{QQ'} \Big|_{\substack{q \to i \\ q' \to i'}} = \underline{\mathcal{G}}_{ii'}^{qq'} \Big|_{\substack{q \to i \\ q' \to i'}} \delta_{Qq,Q'q'} , \tag{52}$$

where the subscript $q \to i$ again means to fix the species q at site i. We gain the insight, that the QQ' matrix $\underline{\mathcal{G}}_{ii'}$ (for i,i' fixed), as expected by its definition, contains only one nonzero element under the condition $q \to i, q' \to i'$ (no averages were taken). Furthermore the connection to the fully averaged $\underline{\mathcal{G}}$ is given by

$$\begin{aligned} \Gamma_{ii}^{QQ'} = \langle \underline{\mathcal{G}}_{ii}^{QQ'} \rangle &= \sum_q c_i^q \langle \underline{\mathcal{G}}_{ii}^{QQ'} \rangle_{q \to i} \delta_{Qq,Q'q} \\ &= c_i^Q \langle \underline{\mathcal{G}}_{ii}^{QQ} \rangle_{Q \to i} \delta_{QQ'} \end{aligned} \tag{53}$$

and

$$\begin{aligned} \Gamma_{ii'}^{QQ'} = \langle \underline{\mathcal{G}}_{ii'}^{QQ'} \rangle &= \sum_{qq'} c_i^q c_{i'}^{q'} \langle \underline{\mathcal{G}}_{ii'}^{QQ'} \rangle_{\substack{q \to i \\ q' \to i'}} \delta_{Qq,Q'q'} \\ &= c_i^Q c_{i'}^{Q'} \langle \underline{\mathcal{G}}_{ii'}^{QQ'} \rangle_{\substack{Q \to i \\ Q' \to i'}} . \end{aligned} \tag{54}$$

In other words the elements of $\underline{\Gamma}$ give the physical two-site conditional averaged Green's matrix connected with the density (26). This just is the gain of using the product Hilbert space.

For the case $c_i^Q = 0$ one gets from Eq. (48) $\underline{b}_{ii}^{QQ} = 0$ and hence $\underline{\mathcal{G}}_{ii}^{QQ} = 0$ independent of $\underline{\Gamma}$. That means, configurations (iQ) with $c_i^Q = 0$ must be removed from the beginning: the set of species Q may depend on the site i in cases of site selectivity.

C. The single-site approximation

Except for the terminal-point approximation for the matrix elements of the Hamiltonian and the overlap matrix, introduced in Sec. III A, we made no approximation in Sec. III so far. In order to solve Eq. (50) we have to introduce an approximation similar to the single-site approximation.[1,2] We require the self-energy to be diagonal in site indices. This leads to a site diagonal inverse scattering potential $\underline{b}$ and we may decouple (50):

$$\underline{T} = (1 - \underline{t}\,\underline{\Gamma}')^{-1} \underline{t}, \quad \underline{t}_{ii'} = \delta_{ii'} (\underline{b}_{ii} - \underline{\Gamma}_{ii})^{-1} , \tag{55}$$

$$\underline{\Gamma}'_{ii'} = (1 - \delta_{ii'}) \underline{\Gamma}_{ii'} \tag{56}$$

with the condition

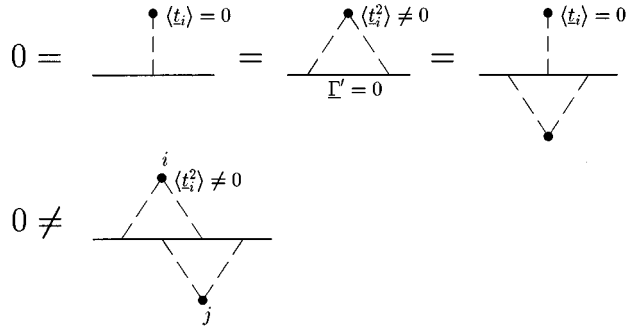

FIG. 1. The diagrams of the first four orders in $\underline{t}$.

$$\langle \underline{t} \rangle \equiv 0 . \tag{57}$$

After expanding the scattering series Eq. (55) and inserting it into Eq. (49) the averaged $\underline{\mathcal{G}}$ becomes

$$\langle \underline{\mathcal{G}} \rangle = \underline{\Gamma} + O(\langle \underline{t}^4 \rangle) \tag{58}$$

as is easily seen in Fig. 1. The final result for the twofold conditional averages in Eq. (26) is then

$$\langle \underline{\mathcal{G}}_{ii}^{Q} \rangle_{Q \to i} = \frac{\Gamma_{ii}^{QQ}}{c_i^Q}, \quad \langle \underline{\mathcal{G}}_{ii'}^{QQ'} \rangle_{\substack{Q \to i \\ Q' \to i'}} = \frac{\Gamma_{ii'}^{QQ'}}{c_i^Q \; c_{i'}^{Q'}}, \tag{59}$$

except for terms of the order $O(\langle t^4 \rangle)$.

This may be a good place for a few comments on the BEB approximation and its quality. As shown here, in the general case of diagonal and off-diagonal disorder, the BEB approximation is formally exact to the same order of the multiple scattering expansion as the CPA is in the case of the diagonal disorder. We have made a number of comparisons with the results of a direct calculation of the projected DOS for one-dimensional model random alloys which indicate an excellent quality of the BEB approximation in a wide range of component bandwidths and other alloy parameters. The alternative treatment of the off-diagonal disorder, the Shiba multiplicative ansatz, can be shown to be a special case of the BEB method, Ref. 28. While the self-consistent equations reduce in number for the Shiba method, an additional calculation is needed to generate the physically and computationally relevant component projected averages $\Gamma_{ii'}^{QQ'}$. For a nonzero overlap matrix, the generalized Shiba matrix factor should be the same for the Hamiltonian and the overlap matrices, and this appears as excessively restrictive for use in realistic calculations. Details of this model analysis will be presented in a separate communication.

In the present paper, we treat consistently the case of several inequivalent sublattices in the elementary cell. For the structure of the self-energy and the validity of the single-site approximation in this case we refer to Appendix A.

IV. THE COMPUTATIONAL SCHEME

In this brief section we summarize the basic features of the present approach, specify the orbital basis used, and give the working equations as they were actually coded and used in the self-consistent computation cycle.

A. General characterization

Any meaningful *ab initio* theory of the electronic structure of alloys should be an extension of a well tested description of the corresponding pure component crystals. In the present case, this is represented by the orbital theory summarized in Ref. 7. In this sense, we continue the earlier work Ref. 9. This early paper served to demonstrate that an orbital CPA need not be a model toy, nor a qualitative semiempirical scheme. Both conceptual and practical limitations restricted the approach to the alloys with near components, like CuNi. By contrast, our present method is sufficiently general.

(1) The present scheme is fully charge self-consistent, all-electron, and, in principle, not restricted by approximations of the atomic-sphere type (additional approximations specified below are not essential). To achieve a wider applicability, we use the scalar relativistic model of Ref. 29.

(2) We use a scattering formulation in the matrix form, which in its general scope parallels the KKR-CPA method. In fact there are similarities with the screened KKR approach.

(3) In the orbital formulation leading to the energy-independent Hamiltonian matrix, the present approach parallels the TB-LMTO-CPA. However, the present approach is not based on the TB transformation, and includes the orbital overlaps.

(4) Both the diagonal and the off-diagonal disorder are included on the same footing in the BEB framework. This opens the possibility to apply it to local basis representations in the most flexible way, including nonorthogonal bases.

(5) The method is formulated so as to incorporate several components and several sub-lattices with different compositions.

B. Orbital basis

Our computational scheme follows the lines of Ref. 7. We are dealing with a minimal basis set of modified orbitals. For each atom the local valence basis is represented by one state per angular momentum and spin. The maximum angular momentum is determined by the type of the element, for transition metals we use s, p, and d states and for actinides up to f states:

$$\langle \vec{r}|\vec{R}\vec{s}nlm\rangle = \phi_{nl}(|\vec{r}-\vec{R}-\vec{s}|)Y_{lm}(\vec{r}-\vec{R}-\vec{s}), \qquad (60)$$

with Y_{lm} being real spherical harmonics. The radial part ϕ does not depend on the magnetic quantum number m. As described, the crystal potential (27) is chosen to be a sum of overlapping site potentials. Additionally, we want to assume the shape of the site potentials to be spherical. This simplification implies that all aspherical parts of the crystal potential are claimed to be approximated by the lattice sum of those spherical site potentials. Surely this is not exact, but for a wide range of applications especially for closed-packed structures this method together with the valence basis treatment as described below has been proved to give results between muffin-tin and full potential approaches. (Aspherical site potentials could be readily incorporated.) First in each self-consistency cycle, the species-dependent basis states are recalculated by solving an atomic Schrödinger or Dirac equation for each atomic species with a potential $V^{Q}_{\vec{R}\vec{s}}$. Details concerning the relativistic implementation of the LCAO method are described elsewhere.[29] $V^{Q}_{\vec{R}\vec{s}}$ is the potential corresponding to the resulting density of the previous cycle. Some atomic potential is used to start with.

While recalculating the core orbitals readily from the site potential $V^{Q}_{\vec{R}\vec{s}}$, the valence basis states will be modified to make them more suitable for the construction of Bloch wave functions. They will be recalculated with an additional attractive potential term $(r/r_0)^4$ which compresses strongly the extended valence states. These compressed states are sufficiently complete in the interstitial region and have a strongly reduced overlap, compared to those calculated from the pure site potential. To close the recalculation of the orbitals these optimized valence orbitals will be orthogonalized to the core states calculated from the pure potential. By this way the number of multicenter integrals is reduced. The parameters r_0 are chosen by convergence checks of the band energies. They scale with the lattice constant and are determined, in principle, by the lattice structure.

C. Implementation of the self-consistent cycle

For the construction of the nonstochastic and hence lattice symmetric Hamilton and overlap matrix we use Bloch sums of AO's in the usual manner resulting in expressions of the form $[\mu=(lm)]$:

$$\underline{\check{H}}^{QQ'}_{\vec{s}\mu,\vec{s}'\mu'}(\mathbf{k}) \quad \text{and} \quad \underline{\check{S}}^{QQ'}_{\vec{s}\mu,\vec{s}'\mu'}(\mathbf{k}), \qquad (61)$$

for the off-diagonal parts (40,42). These **k**-dependent matrix elements together with the elements of the self-energy will be inserted in Eq. (47) to calculate via Brillouin-zone integration the on-site elements of the coherent Green's matrix:

$$\underline{\Gamma}^{QQ'}_{\vec{s},\mu\mu'} = \int_{\mathrm{BZ}} d^3k[\omega-\underline{\Sigma}+\omega\check{S}(\mathbf{k})-\underline{\check{H}}(\mathbf{k})]^{-1}_{\substack{QQ'\\ \vec{s}\mu,\vec{s}\mu'}}. \qquad (62)$$

The off-diagonal elements for $Q\neq Q'$ of the Green's matrix are kept during the self-consistency cycle, but they vanish in the end. Details concerning the crystal symmetry are given in Appendix B. The site diagonal inverse scattering potential $\underline{b}$ (48) can be written as

$$\underline{b}^{QQ'}_{\vec{R}\vec{s}\mu,\vec{R}\vec{s}\mu'} = \sum_q \eta^{q}_{\vec{R}\vec{s}}\,\underline{b}^{(q)QQ'}_{\vec{s},\mu\mu'} \qquad (63)$$

with

$$\underline{b}^{(q)QQ'}_{\vec{s},\mu\mu'} = \delta_{QQ',Qq}(\dot{\underline{H}}^{\,q}_{\vec{s}}-\omega\dot{\underline{S}}^{\,q}_{\vec{s}}+\omega-\underline{\Sigma}^{q}_{\vec{s}})^{-1}_{\mu\mu'}. \qquad (64)$$

To fulfill condition (57) we choose the averaged t-matrix approach. That means, we calculate from Eq. (55) the averaged single-site scattering matrix

$$\langle \underline{t}^{QQ'}_{\vec{s},\mu\mu'}\rangle = \sum_q c^{q}_{\vec{s}}(\underline{b}^{(q)}_{\vec{s}}-\underline{\Gamma}_{\vec{s}})^{-1}_{\substack{QQ'\\ \mu\mu'}}, \qquad (65)$$

which should be zero. The resulting change in the self-energy is $d\underline{\Sigma}=(1+\langle\underline{t}\rangle\underline{\Gamma})^{-1}\langle\underline{t}\rangle$. In an inner CPA self-consistency cycle the Green's matrix, the self-energy and the scattering matrix are recalculated until the averaged single-site scattering matrix vanishes.

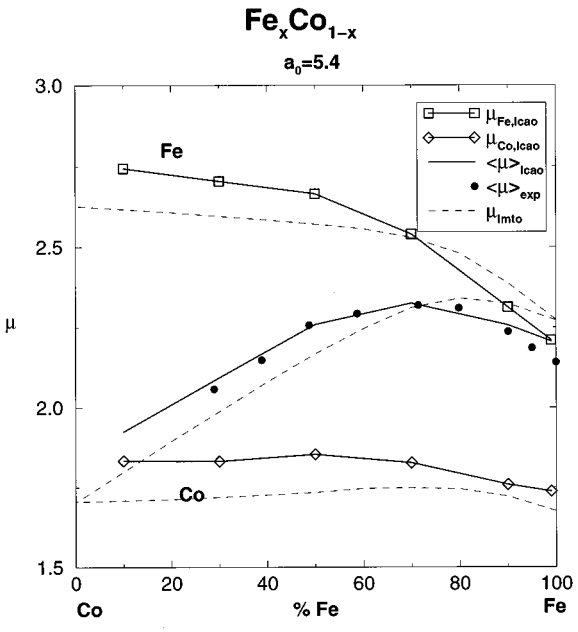

FIG. 2. bcc-FeCo alloy: The dashed lines are the TB-LMTO-ASA result taken from Turek *et al.* The full lines are our results, experimental values are marked by filled symbols.

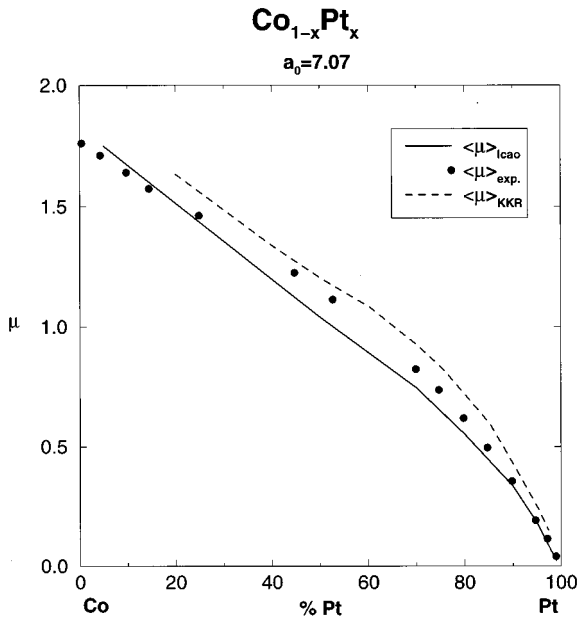

FIG. 3. fcc-CoPt alloy: The dashed line is calculated by the full relativistic KKR-CPA. These data and the experimental values (filled symbols) are reported in Ebert *et al.* Our result is marked by a full line.

To perform the involved ω integration along the real axis accurately, we employ the Herglotz property of the Green's matrix and of related quantities, which allows us to use the common trick of changing the integration contour from the real line to a semicircular path in the upper complex half plane. The integrals depend only on the end points and the functions to be integrated are much smoother far away from the real axis. The integration starts in energy regions below the band bottom and ends at the Fermi energy, which has to be readjusted to get the right number of occupied states.

Once reaching the converged self-energy the energy-integrated Green's matrix elements are inserted into the expression for the density (26). In view of the spherical approximation of site potentials, which is single-site CPA consistent, we compute the spherical average of site densities only. We end up at a density representation consisting of a lattice sum of local spherical, overlapping densities.

This representation of the density leads to the potential via the expressions in Sec. II D. In this way, the self-consistency loop is closed.

V. ILLUSTRATIVE APPLICATIONS

The numerical tests shown below serve to test the reliability and flexibility of our approach. It should be suitable for light and moderately heavy atoms, and for alloys of metals with widely different pure component bandwidths. We present calculations and comparisons for some magnetically ordered binary systems and for a ternary system.

The first example is the bcc FeCo alloy. One main feature of this compound is the transition from filled iron majority bands to lower filling by increasing the iron content, resulting in a maximum of the magnetization curve at 70% Fe concentration. This compound is widely studied. We calculated the magnetization versus concentration at a fixed lattice constant (Fig. 2). For comparison with other methods we present also the LMTO results, published in Ref. 12. Both curves show the characteristic maximum, while our curve is closer to the experimental one. The higher Co moment is consistent with the bcc Co moment obtained by pure LCAO calculations. The deviations to the LMTO result may result from a slightly higher pure Fe moment in their calculations.

The above-mentioned applicability to different bandwidths and relativistic cases is tested in the following two examples. The fcc-CoPt alloy was explored by the fully relativistic KKR method.[30] The magnetization of this compound exhibits a transition to zero moment with increasing Pt concentration. Here the bandwidth of the pure Pt is approximately twice the Co bandwidth. Our scalar relativistic calculation reproduces the slightly nonlinear behavior as given by the KKR results, in good agreement with experiment (Fig. 3).

The last binary example is the Invar alloy fcc FePt, which shows anomalies, for instance in the thermal expansion. The critical region lies between 70% and 80% Pt content. To investigate the nontrivial behavior of the moment and the lattice constant one has to perform total-energy calculations. Here we compare the moments given by our method with those calculated by the recently developed relativistic TB-LMTO-CPA (Ref. 31) at a fixed lattice constant (Fig. 4). (The LMTO data are taken from Ref. 32). Both results show nearly the same local and averaged moments. The experimental data are given in Ref. 33. These three examples prove the applicability of our method in the case of binary alloys.

To show an application to more complicated structures we switch now to a ternary system. The FeAlMn alloys have been known to show interesting and complicated magnetic and structural features. We want to present here theoretical results for the ferromagnetic phase. The composition investigated has the formula $Fe_{0.89-x}Mn_{0.11}Al_x$. When disregard-

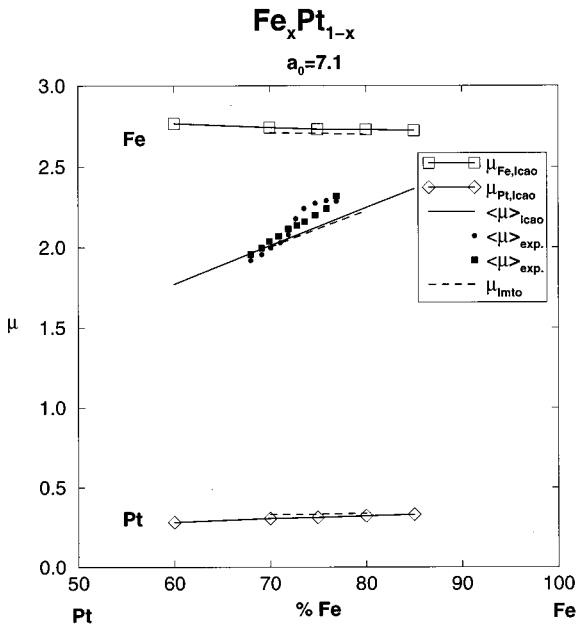

FIG. 4. fcc-FePt alloy: The dashed lines are calculated with the full relativistic TB-LMTO-CPA, developed by Shick *et al.* The full lines are our results, experimental values are marked by filled symbols, they are taken from Wasserman.

ing the different constituents the structure is a bcc ($A2$) lattice. Comparison is made to measurements by Bremers *et al.*[34,35] First we calculated a bcc alloy where each site is randomly occupied. The room-temperature lattice constant was taken from experiment (Bremers) and reduced by 0.5% to the $T=0$ value, estimated from the thermal-expansion coefficient. As can be seen in Fig. 5 and Table I

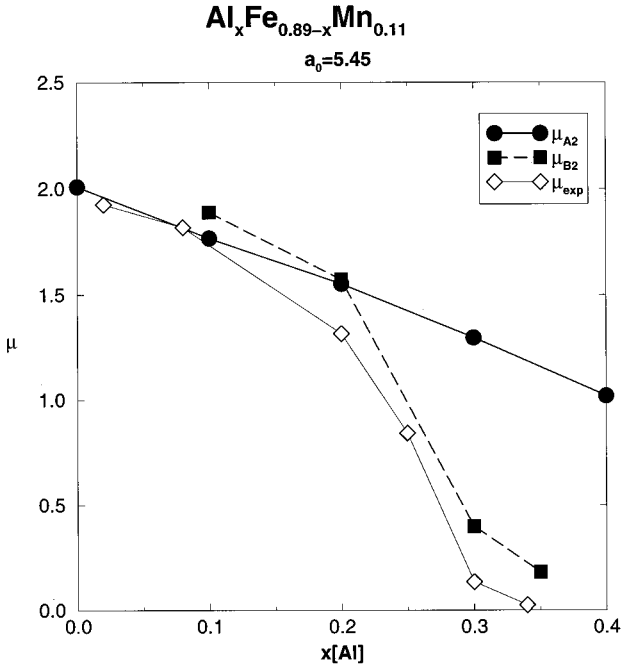

FIG. 5. bcc-FeAlMn alloy: The moment per atom in the ternary bcc alloy for the $A2$ structure and for the $B2$ structure in comparison with experiment. For details see the text.

TABLE I. The local moments and the moment per atom at various Al concentrations for the $A2$ structure of the $Al_xFe_{0.89-x}Mn_{0.11}$ alloy.

x	0.00	0.10	0.20	0.30	0.40
Fe	2.320	2.273	2.185	2.062	1.911
Al		-0.168	-0.150	-0.128	-0.104
Mn	-0.141	-0.118	0.678	1.089	1.135
$\mu_{\text{per atom}}$	2.019	1.766	1.552	1.297	1.019

the values of the averaged magnetization coincide well with the experiment at low Al concentrations. Beyond $x=0.2$ the magnetization at helium temperature is breaking down. This phase transition is not obtained in our ternary CPA treatment of the $A2$ structure. To go a step further we paid attention to the fact, that with increasing Al content experimentally the structure seems to switch to the $B2$ structure. To investigate the influence of this structural long range order on the magnetization we performed a CPA calculation with two simple cubic sublattices, displaced by $(1/2,1/2,1/2)$. One is occupied with pure Fe atoms, the other is occupied with the composition $Fe_{0.78-2x}Mn_{0.22}Al_{2x}$, which corresponds to the ternary alloy with the Al content x. This subdivision is motivated by the observation that in the system AlFe (Ref. 36) (a DO_3 derived structure at $x_{Al}<40\%$) and in similar systems like SiFe(V,Mn),[37,38] the Fe atoms tend to occupy two of the four fcc sublattices of the DO_3 structure. These lattices reduce to the $B2$ structure if one considers the other two sublattices to be equally occupied. We transfer the experimentally known occupation preferences to the $B2$ AlFeMn by assuming one site to carry pure iron atoms. The results are striking. They are collected in Table II. We give the local moments of the two different sites in the $B2$ structure and the moment per atom.

One remarkable feature is easily seen. The local moments of the Fe atoms depend strongly on the nearest-neighbor shell. The Fe atom with eight pure neighbors has a saturated magnetization of about $2.5\mu_B$, while the atom on the Fe sublattice, for which only a small percentage of the eight neighbor atoms are iron, has a reduced moment. This behavior is known from the antistructure atoms in ordered $Fe_{50}Al_{50}$ (Ref. 39) and from the alloys SiFe and SiFeV.[13] Most important, we get a sudden transition of the moment of the pure iron sublattice to ferrimagnetic coupling, thereby enormously reducing the total magnetic moment at about 30%

TABLE II. The local moments of both simple cubic sublattices and the moment per atom at 10, 20, 30, and 35% Al content for the $B2$ structure of the $Fe_{1.0}Al_{2x}Fe_{0.78-2x}Mn_{0.22}$ alloy. The number besides the elements refers to the sublattice.

x	0.10	0.20	0.30	0.35
Fe 1	2.232	1.955	-0.144	-0.274
Fe 2	2.378	2.441	2.592	2.520
Al 2	-0.191	-0.168	0.001	0.014
Mn 2	0.938	1.499	2.167	1.932
$\mu_{\text{per atom}}$	1.890	1.572	0.399	0.181

aluminum. This reduction meets excellently the experimentally observed decrease of the magnetization (Fig. 5).

VI. CONCLUSION

Starting from the local orbital representation of the Kohn-Sham theory we constructed a fully charge and spin self-consistent CPA scheme for calculation of the electronic structure of substitutional disordered alloys. An optimization resulting into a strong localization of the valence orbitals is needed for the assignment of the atoms to the basis states, and for a single atom decomposition of the potential. Even so, the basis states are nonorthogonal. For alloys with very different components, it is essential to treat properly both the diagonal and the off-diagonal disorder both in the overlap matrix and in the Hamiltonian matrix. In our method, this is achieved by the terminal-point approximation, permitting us to achieve the CPA solution within the BEB formalism incorporating a self-consistent recalculation of all matrix elements in each cycle. Among the advantages of the local orbital-matrix representation is a simple inclusion of the scalar relativistic effects and its straightforward applicability to structures with complex unit cells and with a complete or a partial disorder. The numerical results presented have an accuracy comparable with the KKR and LMTO CPA methods currently in use.

To summarize, the pure orbital alternative to the KKR-CPA and to the TB-LMTO-CPA appears as feasible and meaningful. Like the recently developed screened KKR, it combines the rigor and directness of the KKR with the practical simplicity of the LMTO; on top of that its LCAO form provides physically illuminating ''quantum chemical'' insights.

There are several obvious directions for a future work. First, a number of improvements, especially making the construction of the potential more flexible, will be needed to generate a standard computer code, suitable for general use. Within the CPA, several extensions are inevitable, but not difficult to achieve, notably the inclusion of the spin-orbit effects, and the calculation of the total energy as a function of the alloy parameters. A more general question which has arisen during the work is the position of BEB among other alloy formalisms, and the reasons for the unexpected quality of the BEB-CPA.

All this methodological work should not mask the fact that we have developed the present method because it is computationally facile and suitable for the studies of complex alloy structures. We intend to concentrate primarily on this aspect.

ACKNOWLEDGMENTS

We thank J. Kudrnovský and V. Drchal for helpful discussions and for giving us the TB-LMTO-CPA program for comparative calculations. Furthermore we thank M. Richter, J. Forstreuter, and A. Ernst for discussing details concerning the LCAO formalism. Finally, we wish to thank H. Bremers and J. Hesse for providing us with experimental results on the FeAlMn system, partially prior to publication, and for discussions. B.V. acknowledges financial support by the Max-Planck society.

APPENDIX A: THE SELF-ENERGY

Without approximation $\underline{\Sigma}$ is not diagonal in real space. We may write with diagonal invertible $l=\omega\underline{\dot{S}}-\underline{\dot{H}}$ (dropping the underbar):

$$\mathcal{G}=\chi[l-\chi(\Theta-\Gamma^{-1})\chi]^{-1}\chi, \quad \Theta=\omega-\Sigma\,.$$

Corresponding to Eq. (48) one derives (with site diagonal $\lambda=\chi l^{-1}\chi$)

$$\mathcal{G}=\lambda[1-(\Theta-\Gamma^{-1})\lambda]^{-1}=\Gamma+\Gamma T\Gamma,$$

which gives

$$\lambda=(\Gamma+\Gamma T\Gamma)[1-(\Theta-\Gamma^{-1})\lambda]\,,$$

$$T\lambda=(1+T\Gamma)(\Theta\lambda-1), \quad (\langle T\rangle=0)\,.$$

Now we are asking for elements with the right index (called f) being at a site with only one possible occupation. Then, $\langle\lambda_f\rangle=\lambda_f$ holds. The averaging procedure removes terms with $\langle T\rangle$ and yields

$$\Theta_{if}\lambda_f=\delta_{if}\,,$$

$$\underline{\Sigma}_{if}=\delta_{if}[\omega(1-\underline{\dot{S}}_f)+\underline{\dot{H}}_f]\,.$$

Because $\underline{a}$ thus vanishes in the case of fixed site occupation we have to exclude these sites from the CPA equations (50), (57). This general peculiarity of $\underline{\Sigma}$ is preserved in the single-site approximation, where we set by definition all site off-diagonal elements of $\underline{\Sigma}$ to zero. It gives us hope to expect that the CPA would be better if less stochastic sites existed in the unit cell.

APPENDIX B: THE BRILLOUIN-ZONE INTEGRATION

In order to calculate the on-site elements of the coherent Green's matrix $\underline{\Gamma}^{QQ'}_{s,\mu\mu'}$ we perform Brillouin-zone integrations over $\underline{\Gamma}^{QQ',\mathbf{k}}_{s,\mu\mu'}$. To reduce this time consuming step it is unavoidable to integrate only in the irreducible part of the BZ. Unfortunately, we have to symmetrize the Green's matrix after doing so, because $\underline{\Gamma}^{\mathbf{k}}$ does not form a unit representation of the full Brillouin-zone symmetry. In simple cases, like unit cells where each site has the full cubic symmetry and with basis states up to d states, this task is very easy. Then $\underline{\Gamma}^{QQ'}_{s,\mu\mu'}$ is diagonal in $\mu\mu'$ and the matrix elements for given angular momentum l are m degenerated. The average over all diagonal elements to a fixed l gives just the desired symmetrization of $\underline{\Gamma}$ calculated by integration over the irreducible part of the Brillouin zone.

For more complicated crystals we outline the treatment. Let us start with the definition of the space-group operation $\hat{U}=\{u|\tau\}$, where we used the symbol after Seitz for the operation which takes a point at $\mathbf{r}$ to $\mathbf{r}'=\hat{U}\mathbf{r}=u\mathbf{r}+\tau$. u means a point-group operation, a proper or improper rotation, while τ is a translation through a vector. It can be a composite of a primitive lattice translation $\vec{R}$ and of an essential nonprimitive translation τ_0, which in cases of nonsymmorphic space

groups can never be made to vanish by shifting the origin: Ref. 40. The set of symbols $\{u|\tau_0\}$ with τ_0 being a specified set of nonprimitive translation vectors does not form itself a subgroup in nonsymmorphic space groups. We therefore consider the vectors τ as general composits of primitive and nonprimitive lattice vectors. This ensures the group properties of the symbols $\{u|\tau\}$.

The action of these operations on the LCAO basis states is given by

$$\hat{U}|\vec{R}\vec{s}\mu\rangle=\sum_{\mu'}|\hat{U}(\vec{R}+\vec{s})\mu'\rangle a_{\mu'\mu}. \tag{B1}$$

The coefficients a are representation matrices of the point-group element u for an angular momentum l and provide the transformation of the spherical harmonics included in the basis states. This relation holds for arbitrary space groups. Together with the transformation properties of the phase factor $\exp(i\mathbf{k}\vec{R})$ we deduce

$$\underline{\Gamma}^{QQ',u^\dagger\mathbf{k}}_{\vec{s},\mu\mu'}=\sum_{\nu\nu'}a^*_{\nu\mu}\underline{\Gamma}^{QQ',\mathbf{k}}_{\hat{U}\vec{s},\nu\nu'}a_{\nu'\mu'} \tag{B2}$$

holding for site diagonal elements only. This formula is valid for arbitrary space groups. Note, that a space-group operation $\hat{U}$ acts on $\vec{s}$, while only the corresponding point-group element u acts on $\mathbf{k}$. Now we decomposed the integral in the whole zone into a sum over integrals in the irreducible part but over rotated matrices, u represents all point-group operations:

$$\underline{\Gamma}^{QQ'}_{\vec{s},\mu\mu'}=\int_{\mathrm{BZ}}d^3k\underline{\Gamma}^{QQ',\mathbf{k}}_{\vec{s},\mu\mu'} \tag{B3}$$

$$=\sum_{\hat{U}}\int_{\mathrm{ir\,BZ}}d^3k\underline{\Gamma}^{QQ',u^\dagger\mathbf{k}}_{\vec{s},\mu\mu'}. \tag{B4}$$

The sum runs over all space-group elements. Examining the symmetry relations (B2) we get

$$\underline{\Gamma}^{QQ'}_{\vec{s},\mu\mu'}=\sum_{\hat{U}}\int_{\mathrm{ir\,BZ}}d^3k\sum_{\nu\nu'}a^*_{\nu\mu}\underline{\Gamma}^{QQ',\mathbf{k}}_{\hat{U}\vec{s},\nu\nu'}a_{\nu'\mu'} \tag{B5}$$

$$=\sum_{\vec{s}',\nu\nu'}\underline{\Gamma}^{QQ'(\mathrm{ir\,BZ})}_{\vec{s}',\nu\nu'}\sum_{\hat{U}\vec{s}=\vec{s}'}a^*_{\nu\mu}a_{\nu'\mu'}. \tag{B6}$$

The space-group operations can be classified by inspecting the pairs of basis vectors $\vec{s}$, $\vec{s}'$ which are transformed into another. There exists for each $\vec{s}'$ a possibly empty subset of $\hat{U}$'s which transforms a given vector $\vec{s}$ into $\vec{s}'$: $\vec{s}'=\hat{U}\vec{s}\,\mathrm{mod}\{\vec{R}\}$. For a specified $\vec{s}$, the union of the subsets belonging to all basis vectors $\vec{s}'$ in the unit cell contains each group operation exactly once. Thus, the second sum in Eq. (B6) runs over the set of group operations which transform $\vec{s}$ into $\vec{s}'$. The superscript on $\underline{\Gamma}$ denotes the $\mathbf{k}$ integration over the irreducible part. Since the last sum in Eq. (B6) is only structure dependent it is performed once for ever and then the symmetrization is much faster than to calculate $\underline{\Gamma}^{\mathbf{k}}$ for each $\mathbf{k}$ point in the whole zone.

*Permanent address: Charles University, Prague, Czech Republic.

[1] P. Soven, Phys. Rev. **156**, 809 (1967).
[2] D. W. Taylor, Phys. Rev. **156**, 1017 (1967).
[3] B. Velický, S. Kirkpatrick, and H. Ehrenreich, Phys. Rev. **175**, 747 (1968).
[4] G. M. Stocks, W. M. Temmermann, and B. L. Gyorffy, Phys. Rev. Lett. **41**, 339 (1978).
[5] M. Schröter *et al.*, Phys. Rev. B **52**, 188 (1995).
[6] O. K. Andersen and O. Jepsen, Phys. Rev. Lett. **53**, 2571 (1984).
[7] H. Eschrig, *Optimized LCAO Method and the Electronic Structure of Extended Systems* (Springer, Berlin, 1989).
[8] J. Kudrnovský, V. Drchal, and J. Masek, Phys. Rev. B **35**, 2487 (1987).
[9] R. Richter, H. Eschrig, and B. Velický, J. Phys. F **17**, 351 (1987).
[10] R. Richter and H. Eschrig, J. Phys. F **18**, 1813 (1988).
[11] R. Richter and H. Eschrig, Phys. Scr. **37**, 948 (1988).
[12] I. Turek, J. Kudrnovský, V. Drchal, and P. Weinberger, Phys. Rev. B **49**, 3352 (1994).
[13] J. Kudrnovský, N. E. Christensen, and O. K. Andersen, Phys. Rev. B **43**, 5924 (1991).
[14] J. Kudrnovský, S. K. Bose, and O. K. Andersen, Phys. Rev. B **43**, 4613 (1991).
[15] R. Zeller *et al.*, Phys. Rev. B **52**, 8807 (1995).
[16] H. Shiba, Prog. Theor. Phys. **46**, 77 (1971).
[17] J. Kudrnovský and J. Mašek, Phys. Rev. B **31**, 6424 (1985).
[18] I. A. Abrikosov and H. L. Skriver, Phys. Rev. B **47**, 16 532 (1993).
[19] J. Kudrnovský *et al.*, Phys. Rev. B **47**, 16 525 (1993).
[20] J. A. Blackman, D. M. Esterling, and N. F. Berk, Phys. Rev. B **4**, 2412 (1971).
[21] D. A. Papaconstantopoulos, A. Gonis, and P. M. Laufer, Phys. Rev. B **40**, 12 196 (1989).
[22] A. Mookerjee, J. Phys. C **6**, 1340 (1973).
[23] A. Gonis and J. W. Garland, Phys. Rev. B **16**, 1495 (1977).
[24] A. V. Ruban, I. A. Abrikosov, and H. L. Skriver, Phys. Rev. B **51**, 12 958 (1995).
[25] P. A. Korzhavyi, A. V. Ruban, I. A. Abrikosov, and H. L. Skriver, Phys. Rev. B **51**, 5773 (1995).
[26] G. Schadler, P. Weinberger, A. Gonis, and J. Klima, J. Phys. F **15**, 1675 (1985)
[27] J. Phillips and L. Kleinman, Phys. Rev. **116**, 287 (1959).
[28] J. A. Blackman, J. Phys. F **3**, L31 (1973).
[29] M. Richter and H. Eschrig, Solid State Commun. **72**, 263 (1989).
[30] H. Ebert, B. Drittler, and H. Akai, J. Magn. Magn. Mater. **104-107**, 733 (1992).
[31] A. B. Shick, V. Drchal, J. Kudrnovský, and P. Weinberger, Phys. Rev. B **54**, 1610 (1996).
[32] A. B. Shick, V. Drchal, and J. Kudrnovský (private communication).
[33] E. F. Wasserman, in *Ferromagnetic Materials*, edited by K. H. J. Buschow and E. P. Wohlfarth (North-Holland, Amsterdam, 1990), Vol. 5, p. 237.
[34] H. Bremers, C. Jarus, and J. Hesse, J. Magn. Magn. Mater. **140-144**, 63 (1995).
[35] H. Bremers, C. Jarus, and J. Hesse (private communication).

[36] J. G. Booth, in *Ferromagnetic Materials*, edited by K. H. J. Buschow and E. P. Wohlfarth (North-Holland, Amsterdam, 1988), Vol. 4, p. 211.
[37] T. J. Burch, T. Litrenta, and J. I. Budnick, Phys. Rev. Lett. **33**, 421 (1974).
[38] J. I. Budnick, Z. Tan, and D. M. Pease, Physica B **158**, 31 (1988).
[39] Y. M. Gu and L. Fritsche, J. Phys. Condens. Matter **4**, 1905 (1992).
[40] T. Inui, Y. Tanabe, and Y. Onodera, *Group Theory and its Applications in Physics* (Springer, Berlin, 1990), p. 234.